IEEE Access
Multidisciplinary ⋮ Rapid Review ⋮ Open Access Journal

Received November 30, 2019, accepted January 13, 2020, date of publication January 17, 2020, date of current version January 27, 2020.

Digital Object Identifier 10.1109/ACCESS.2020.2967059

Simultaneous Stiffness Measurement Device for a Human Forearm

DONGHOON OH[1], SEULAH LEE[2], AND YOUNGJIN CHOI[2], (Senior Member, IEEE)

[1]Neuromeka Company, Daejeon 34113, South Korea
[2]Department of Electrical and Electronic Engineering, Hanyang University, Ansan 15588, South Korea

Corresponding author: Youngjin Choi (cyj@hanyang.ac.kr)

This work was supported by the Convergence Technology Development Program for Bionic Arm through the National Research Foundation of Korea funded by the Ministry of Science, ICT and Future Planning, South Korea, under Grant NRF-2015M3C1B2052811.

ABSTRACT The paper proposes a stiffness measurement device composed of a measurement part that includes four indenters and an arm anchorage part that includes four linear servomotors. The device is able to make simultaneous stiffnesses measurements of the human forearm. An indenter using parallelogram mechanisms has two degrees-of-freedom and is designed to measure the stiffness at various locations. The kinematics of the parallelogram mechanism is computed to control the position of the indenters. Additionally, the admittance compensator for force control is designed so that the indenter can press the skin surface of the human forearm. According to the force level measured at loadcell installed on the indenter, the control is switched between pure position control and admittance control. Further, this device includes a two-axis potentiometer at the indenter endpoint. This potentiometer acts like a passive two degrees-of-freedom universal joint, allowing the indenter to press perpendicular to the measurement skin area. For this purpose, the mapping between the voltage output and the potentiometer angle was obtained by fitting for each axis. The proposed measurement device was tested for accuracy and repeatability. Ultimately, the measurement device was able to measure the stiffnesses of four regions of the human limb simultaneously.

INDEX TERMS Multi-indenter, parallelogram mechanism, admittance control, prosthetic socket, human forearm stiffness.

I. INTRODUCTION

Human limbs are important for conducting various physical activities for daily life, but the number of amputees in the United States has been increasing steadily and is estimated to reach more than 3.6 million in 2050 [1]. As the number of amputees increases, prosthetic industries have introduced the improved technologies such as robotics and bionics. Some significant factors to consider when developing prostheses are the function, weight, wearability for users, and having a low-cost. Especially, prosthetic sockets have been studied in a variety of fields, including orthopedics, rehabilitation medicine, and medical engineering [2]–[6]. A prosthetic socket is a component that connects the residual limb of the amputee to the prosthesis. Unfortunately, the prosthetic socket is still handcrafted by a prosthetist, and thus, it is difficult to maintain the quality of the sockets because there is no standardized method for their manufacturing yet. Additionally, sockets are usually tightly wrapped around the residual limb so that they are firmly fixed [7], [8]. For these reasons, many prosthetic users suffer from fatigue, inconvenient wearability, inflammation, and tissue damage as side effects [9], [10]. Moreover, compressive loading between bone structures and prosthesis is a critical issue for designing prosthetic sockets.

To resolve these aforementioned issues, researchers have been studying prosthetic sockets from the viewpoint of residual limb stiffness around the prosthetic socket [11]–[14]. The proposed measurement device offers useful information in making the customized sockets for amputees. Furthermore, the biomechanical data and model acquired using the stiffness measurement device could provide important information related to sports clothing, shoes, and prostheses which can be applied to human limbs through mechanical loads [15], [16].

Stiffness measurement devices for human limbs have gradually been an interesting topic regarding advanced prosthesis. In recent studies on such devices, Petron *et al*. [11] developed a multi-indenter device that has a total of fourteen indenters surrounding the measurement site. Eleven of these indenters were used to anchor the measurement site and the remaining

The associate editor coordinating the review of this manuscript and approving it for publication was Wuliang Yin.

three indenters were used to measure the stiffness of the human limb. However, this approach has a disadvantage in that the undesired forces are transmitted to the measurement site because the limb anchorage was operated at the measurement site. Indeed, the forces caused by the eleven indenters for the anchorage can deform the measurement site. In addition, a universal joint with two passive DoFs (degrees-of-freedom) was equipped at the endpoint of the indenter so that indentation could be made vertically when in contact with the skin surface. However, the direction of the force provided by the indenter and the direction in which the indenter is pressed onto the skin to measure this force are different from each other. Samur *et al*. [17] proposed a robotic indenter to measure tissue properties for minimally invasive surgery. Although this robotic indenter was able to obtain various tissue information, it did not have any joints to guarantee vertical loading onto the skin, *i.e.,* it cannot be used to obtain information for making prosthetic sockets. Pathak *et al*. [18] have developed a tissue testing system to assess *in vivo* compressive loading on residual limb tissue. This testing system is portable and composed of a linear actuator, load cell, casing and guides, and a mechanical safety device, but only a single indenter with one DoF. Further, the residual limb circumference could not be measured simultaneously. Likewise, most existing studies mainly focused on tissue measurements.

As an alternative, herein we develop a stiffness measurement device with a two-axis potentiometer attached to the endpoint of the indenter. The proposed device is used to estimate the actual indentation force by measuring the angle between the normal direction of the measurement skin site and the force direction of the indenter. The aforementioned existing indenters have only one DoF [8]–[11], [17], [18], but the developed indenter has two active DoFs and a passive joint that allows vertical indentation onto the skin. Additionally, the measurement system suggested in [11] was uncomfortable when measuring the stiffness because the subject would have to move their own limb whenever the measurement site changed. However, the proposed device is able to move the location of the indenter toward the target site using the parallelogram mechanism.

Therefore, the aim of this paper is to develop a multi-intender device using the parallelogram mechanisms not only for the simultaneous measurements of the stiffnesses according to the circumference of the human forearm, but also for changing the indenter locations without moving the human forearm. For these purposes, the developed device including four 2-DoF indenters was designed for collecting the data regarding the residual limb measurement, ultimately for the customized sockets. To verify the performance of the proposed measurement device, first experiments are conducted using the springs with known stiffnesses. Through these experiments, we confirm the accuracy of the proposed device, and then the stiffnesses of the human limb are measured according to the circumference and length of the forearm as the main experiments.

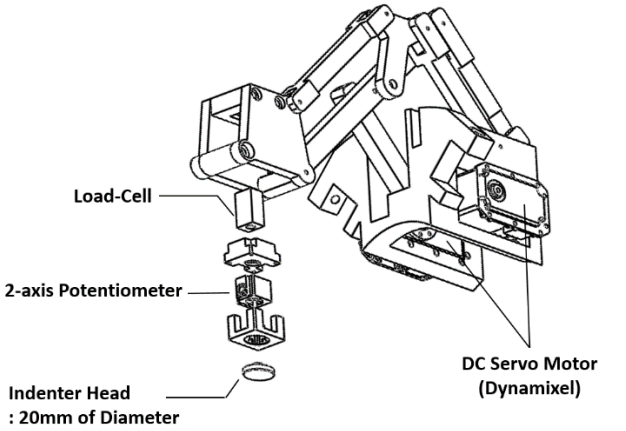

FIGURE 1. Structure of the indenter located on the measurement part. The indenter position is controlled using two rotary servomotors. The indenter consists of a loadcell to measure the indentation force, a 2-axis potentiometer to measure the indentation direction, and an indenter head to press the skin.

This paper is organized as follows: the mechanism design of the measurement device is presented in Section II, experimental results and discussions about the experimental results are given in Section III, and conclusions are drawn in Section IV.

II. DESIGN OF THE MEASUREMENT DEVICE

The proposed measurement device is composed of four indenters operated by parallelogram mechanisms, electrical circuits to power the indenters, and a control system. These components are explained in the following sections.

A. INDENTER

The indenter module of the developed measurement device is illustrated in Fig. 1. The 2-DoF indenter is driven by two rotary servomotors using the parallelogram mechanism. The planar parallelogram mechanism for the skin indentation was adopted with three purposes; the one is because it is able to maintain the constant orientation of the end-effector that presses in the direction perpendicular to the skin of the forearm irrespective of the active joint movements, another is because the electric servomotors can be installed in the fixed-base, and the other is because it is able to measure the stiffnesses at various locations in one measurement cycle without moving the forearm of the subject. As shown in Fig. 2, the parallelogram mechanism allows the end-effector of the indenter to perform only translational movements without any rotational movement due to the mechanism characteristics generated by the subordinate links, which are denoted by green lines in the figure. In addition, the position of the end-effector is determined by the main links, which are denoted by red lines in the figure, as suggested in [19]. Therefore, the indenter can measure the indentation force along the Y-axis direction as depicted in the figure while maintaining the constant posture, regardless of the position along the X-axis.

The active joints driven by two rotary servomotors are placed on the fixed-base, and the global coordinate frame is

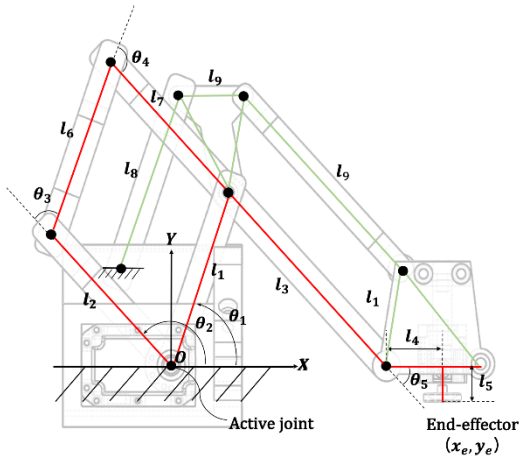

FIGURE 2. Indenter using the parallelogram mechanism with an *X-Y* coordinate frame, where l_1=l_2=l_6=l_7=l_8=0.09[m], l_3=l_9=0.12[m], l_4=0.02993[m], and l_5=0.017[m].

attached to the fixed-base, expressed by OXY in Fig. 2. The angles of the active joints are denoted by θ_1 and θ_2 in Fig. 2, and θ_3, θ_4 and θ_5 can be obtained as the functions of active joint angles θ_1 and θ_2. To determine the position of the end-effector, denoted by x_e and y_e, as functions of the angles θ_1 and θ_2, the forward kinematics for the mechanism is derived from Fig. 2 as follows:

$$\begin{aligned} x_{\mathbf{e}} &= l_1 \cos\theta_1 - l_3 \cos\theta_2 + l_4 \\ y_{\mathbf{e}} &= l_1 \sin\theta_1 - l_3 \sin\theta_2 - l_5 \end{aligned} \tag{1}$$

where l_1 and l_3 denote the link lengths that affect the kinematics, and θ_1 and θ_2 express the active joint angles that operate using two rotary servomotors as suggested in Fig. 2. On the other hand, the inverse kinematics can be calculated from Eq. (1). To obtain θ_1 and θ_2 from any specified position of the end-effector, we introduce a new variable defined by $\alpha = \theta_2 - \theta_1$ as follow:

$$\alpha = \cos^{-1}\left(\frac{l_1^2 + l_3^2 - (x_e - l_4)^2 - (y_e + l_5)^2}{2 l_1 l_3}\right)$$

which allows us to write the inverse kinematic solution. For this purpose, let us begin with following equation:

$$\begin{aligned} x_e - l_4 &= l_1 \cos\theta_1 - l_3 \cos(\theta_1 + \alpha) \\ &= [l_3 \sin\alpha] \sin\theta_1 + [l_1 - l_3 \cos\alpha] \cos\theta_1 \end{aligned}$$

After applying $A \sin\theta + B \cos\theta = \sqrt{A^2 + B^2} \sin(\theta + \tan^{-1}\frac{B}{A})$, we have

$$\begin{aligned} \theta_1 &= \sin^{-1}\left(\frac{x_e - l_4}{\sqrt{l_1^2 + l_3^2 - 2 l_1 l_3 \cos\alpha}}\right) \\ &\quad - \tan^{-1}\left(\frac{l_1 - l_3 \cos\alpha}{l_3 \sin\alpha}\right) \\ \theta_2 &= \theta_1 + \alpha \end{aligned} \tag{2}$$

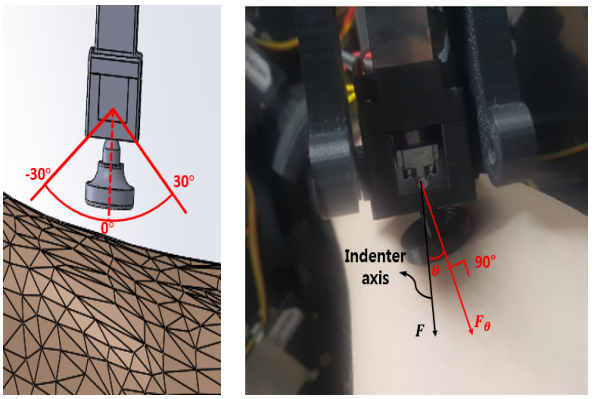

FIGURE 3. Two-axis potentiometer attached to the endpoint of the indenter.

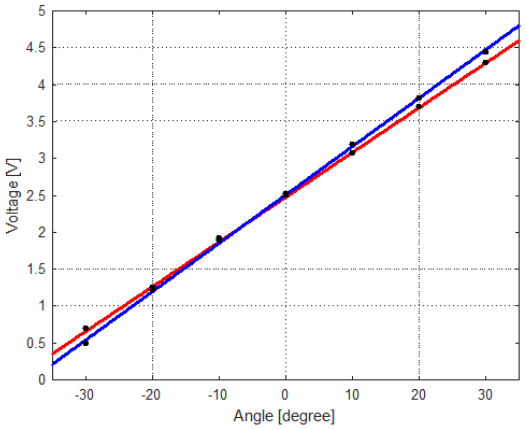

FIGURE 4. Relationship between the angular variations of a potentiometer attached on the indenter's endpoint and its output voltages, and their linear fittings, where the R-squared (R^2) of x-axis and z-axis for the potentiometer were 0.9990 and 0.9994, respectively, and R^2 expresses a statistical measure that represents the proportion of the variance for the dependent variables in a regression model.

where $0 \leq \theta_2 \leq \pi$, $0 \leq \theta_1 \leq \frac{\pi}{2}$, and $\theta_2 > \theta_1$. Indeed, above solutions of the inverse kinematics are used to determine the desired joint angles θ_{d1} θ_{d2} to be applied to two rotary servomotors from the desired position of the end-effector x_d y_d.

As shown in Fig. 3, a two-axis potentiometer is attached to the end-effector, which acts like a 2-DoF passive joint with the driving range of –30 to 30 degrees about each axis. To precisely calculate the perpendicular force with which the indenter presses onto the forearm, the two-axis potentiometer is used to measure the angular differences between the normal direction of the skin and the indenter axis.

Linear fitting for the two-axis potentiometer is performed using the data measured between the angle and the voltage output, as shown in Fig. 4. The R-squared (R^2) values between the linear fitting equation and the angle-voltage data were 0.9990 and 0.9994 about the x-axis and z-axis of the potentiometer, respectively. Since these R^2 values indicate high reliability, the angular differences between the normal

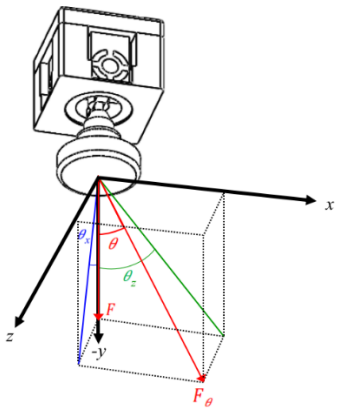

FIGURE 5. Configurations of angle and force generated at the endpoint according to 2-DoFs passive motion of the potentiometer, where the coordinate system of two-axis potentiometer was assigned.

direction of the forearm skin and the indenter axis can be exactly measured. The configurations of the angle and force are generated at the end-effector according to the 2-DoF passive motion of the potentiometer, as shown in Fig. 5. The force perpendicular to the skin is denoted by F_θ, which is the actual force applied to the skin, but it cannot be directly measured. Thus, the force F is measured based on the load-cell and the direction of the indenter. In addition, the angles θ_x and θ_z are measured as the deviation angles from x-axis and z-axis directions, respectively, using the potentiometer. As a result, F_θ applied to the skin is calculated as follows:

$$F_\theta = \frac{F}{\cos\theta} \tag{3}$$

where θ is the angle between the indenter axis and the direction perpendicular to the skin, as denoted in Fig. 5. In other words, the normal force F_θ applied to the skin is now calculated using the following equation:

$$F_\theta = F\sqrt{\tan^2\theta_x + \tan^2\theta_z + 1} \tag{4}$$

because $\cos\theta$ is calculated as the square root of $(\tan^2\theta_x + \tan^2\theta_z + 1)$ using the deviation angles θ_x and θ_z. As a result, the force perpendicular to the forearm skin is obtained using three variables: the load-cell force F, and the deviation angles θ_x and θ_z from the potentiometer. This force is in turn used to calculate the stiffness of the human forearm.

The stiffness measurement device of the forearm is two-layered, including a measurement part and an arm anchorage part as shown in Fig. 6, in order to minimize the influence of changes in the skin and soft tissue. The measurement part has a total of four indenters arranged at intervals of 90 degrees so that the indenters can press onto the forearm uniformly. In addition, the arm anchorage part operated by four linear servomotors, reduces the artifacts that might be caused by forearm movement in the four directions.

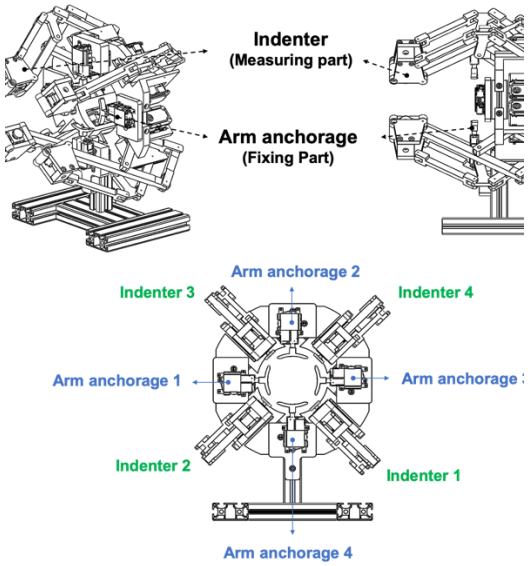

FIGURE 6. Stiffness measurement device composed of the measurement part including four indenters.

TABLE 1. Electromechanical components of the system.

component	parameter	value
two-axis potentiometer (RKJXK122000D, Alps Electric Co., Japan)		-30~30°
rotary servomotor with absolute encoder (Dynamixel MX-64R, ROBOTIS Co., Korea)	Deg/pulse	0.0879
linear servomotor (mightyZAP, IR ROBOT Co., Korea)		27[mm]

B. ELECTROMECHANICAL COMPONENTS

Specifications for the electromechanical components of the measurement device are listed in Table 1 and presented as follows: host computer; microcontroller [OpenCM 9.04-C, ROBOTIS Co., Korea] & [Arduino Leonardo, Arduino.cc, Italy]; RS-485 transceiver for OpenCM 9.04-C [OpenCM 485 EXP, ROBOTIS Co., Korea]; RS-485 transceiver for Arduino Leonardo [IR-STS01, IR ROBOT Co., Korea]; two-axis potentiometer [RKJXK122000D, Alps Electric Co., Japan]; rotary servomotor with absolute encoder [Dynamixel MX-64R, ROBOTIS Co., Korea]; and linear servomotor (27mm stroke) [mightyZAP, IR ROBOT Co., Korea].

The rotary servomotor (Dynamixel) used in the indenter of the proposed measurement device has an absolute encoder so that the current position can be obtained without initialization. Also, it has a PID position controller embedded inside the rotary servomotor and built-in torque limit function for guaranteeing the safety of human users. With a built-in PID position controller, each indenter is controlled to the desired angles after solving the inverse kinematics. Furthermore,

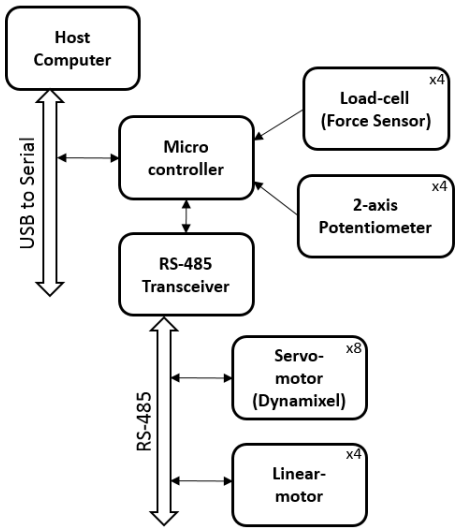

FIGURE 7. **Communication diagram between electrical components in the stiffness measurement device.**

the linear servomotor of the arm anchorage part has a built-in force limit function that helps anchor the forearm in place with the desired force as well as guarantee the safety of human users.

C. CONTROL SYSTEM

Fig. 7 shows a communication diagram between the electrical components in the stiffness measurement device. All commands are executed on the host computer using a C++ based controller program. The customized controller program is able not only to control each indenter by sending commands related to the desired position x_d y_d or the desired force F_d of each indenter through the microcontroller, but also adjust the arm anchorage part to hold the forearm firmly. In more detail, the microcontroller receives commands from the host computer and sends the desired joint angles θ_{d1} θ_{d2} to all rotary servomotors in the measurement device via the RS-485 transceiver. Initially, the linear servomotors are used to fasten the forearm with the specified force limits along the four directions, and then the rotary servomotors are operated to measure the regional stiffnesses of the forearm. During all processes, data on the forearm stiffnesses are acquired from the load-cells, 2-axis potentiometers, and absolute encoders mounted in the rotary servomotors.

The entire control scheme for the indenter using the parallelogram mechanism is illustrated in Fig. 8. The force measured from load-cell is utilized to switch between the desired position of the end-effector and the output of admittance controller in the y-axis direction. In other words, the switching unit (denoted by Switching in Fig. 8 determines the desired position according to the measured force level. Additionally, the forward and inverse kinematics of Eqs. (1) and (2) are utilized to calculate the actual position of the end-effector and the desired joint angles, respectively. Finally, the desired joint angles are applied to the rotary servomotors through RS-485 communication. The rotary servomotor has an internally embedded PID position controller as mentioned before, and thus the admittance controller should be designed to transform the desired force into the desired position variation. For the embedded PID controller, a proportional gain was set to 850, an integral gain to 1 and a derivative gain to 10 through trial and error by experiences. The C++ based host controller utilizes multi-tasking threads, and each task is implemented through communication between the components, reading sensor values, and calculating the desired joint angles for the servomotors.

For the admittance compensator denoted in Fig. 8, the following relationship between the force difference and the y-axis position variation is utilized:

$$F_e = b\Delta\dot{y} + k\Delta y \tag{5}$$

where F_e is the force difference between the actual force measured from the load-cell and the desired force commanded by the user, and $\Delta\dot{y}$ and Δy denote the velocity and position variations, respectively, that are added to the actual y-axis position of the end-effector obtained from the forward kinematics. To implement Eq. (5) in the discrete-time domain, the velocity variation (denoted by $\Delta\dot{y}$) is obtained after applying a lowpass filter and taking the time derivative of the position variation. For this purpose, the time constant of the lowpass filter is set to 0.1[s], the sampling time to 0.001[s], the coefficient b to 3.5[Ns/mm], and the coefficient k to 0.18[N/mm]. Note that these coefficients are found through trial and error. The admittance compensator in the discrete-time form of Eq. (5) yields the position variation Δy from the force difference F_e, which is ultimately applied to the position controller embedded inside the rotary servomotor.

D. EXPERIMENTAL SETUP

This study was approved by the Institutional Review Board (IRB) on Human Subjects Research and Ethics Committee at Hanyang University Hospital, Seoul, Korea (2018 July, HYI-16-055-3). To verify the performance of the proposed stiffness measurement device, three kinds of experiments are conducted. First, the stiffness of the actual spring is measured using the indenter. Known springs with different stiffnesses (stiffness coefficients of 0.5N/mm and 1N/mm) are used, and each spring is measured five times with 1N increments from 1N to 5N, to verify the accuracy of the proposed stiffness measurement device. Second, all the indenters make measurements of the same skin areas on the human forearm three times each. A sufficient time interval between each indentation process is required to alleviate the hysteresis effect of human skin, and the repeatability of the measurement device is verified experimentally as well. Finally, the regional stiffnesses of the human forearm are measured for thirteen participants because trans-radial amputation is more common than trans-humeral amputation [20]. In addition, we tried to take measurements of the participant forearms while maintaining the same skin conditions.

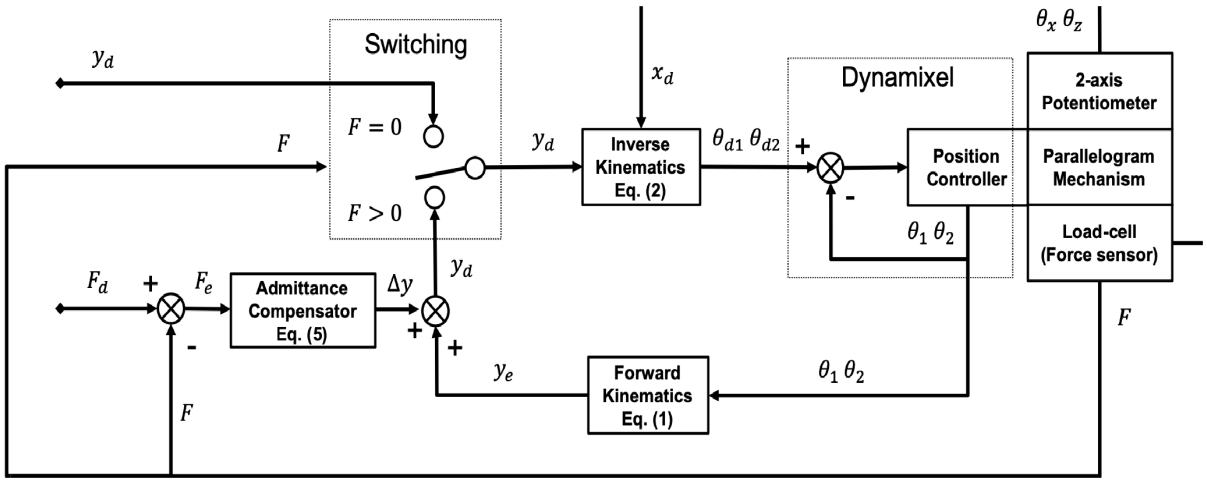

FIGURE 8. Entire control diagram for the indenter, where Switching represents the selection process according to the force, x_d and y_d express the desired x-axis and y-axis values of the end-effector, respectively, F_d denotes the desired force, θ_{d1} and θ_{d2} are the desired joint angles to be assigned to the position controller, and θ_1 and θ_2 the actual joint angles.

As a first step for measuring the forearm stiffness, the operator enters a command to operate the arm anchorage part through the host computer so that the four linear servomotors can fasten themselves to the human wrist. As a second step, the experimenter enters the command to move the four indenters to the positions of 70[mm] and 120[mm] away from the arm anchorage part, as shown in Fig. 9(a). After confirming that the wrist is firmly anchored, all indentation forces applied to the skin areas are set to 5[N], and indentation experiments are repeatedly conducted to determine the force-distance relationship and ultimately to calculate the stiffness of the corresponding forearm area. After completing all the measurements, the return command signal is entered by the experimenter so that the four indenters and four linear servomotors can be separated from the forearm, returning to their initial positions. While pressing the forearm, passive joint angles of two-axis potentiometers are measured to determine the force normal to forearm skin.

III. RESULTS AND DISCUSSIONS

Control of the indenter using the parallelogram mechanism was implemented to verify the proposed stiffness measurement system. To confirm the accuracy and repeatability of the proposed indenter mechanism, the spring coefficients were measured by the indenter in such a way that two springs with the known coefficients of 0.5[N/mm] and 1[N/mm] were tested, as shown in Fig. 10(a). The mean values of the spring coefficients measured using the developed device were 0.491[N/mm] and 0.943 [N/mm], respectively, exhibiting only small errors. As a result, when the spring coefficients were measured repeatedly using the proposed device, neither value deviated much from the actual spring coefficients, regardless of the force change within the limited range. In other words, the proposed device showed good accuracy and repeatability during device verification.

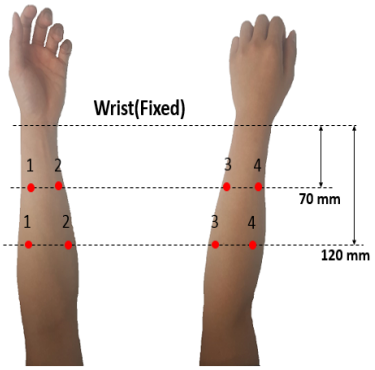

(a) four measurement points for stiffness measurements of the forearm, which were chosen to be 70[mm] and 120[mm] away from the wrist (the arm anchorage part)

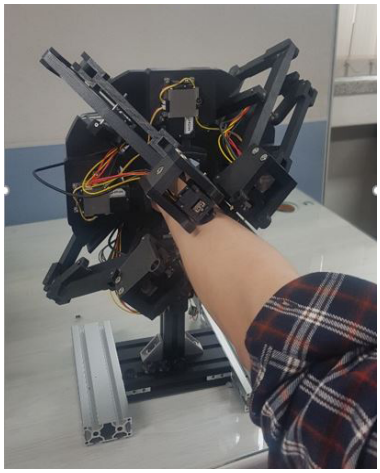

(b) snapshot of the actual experiment while making measurement of the forearm stiffness

FIGURE 9. Experimental setup for human forearm.

For the main experiments, the stiffnesses are simultaneously measured using the indentation displacements and forces applied to the four points on the forearm. The desired

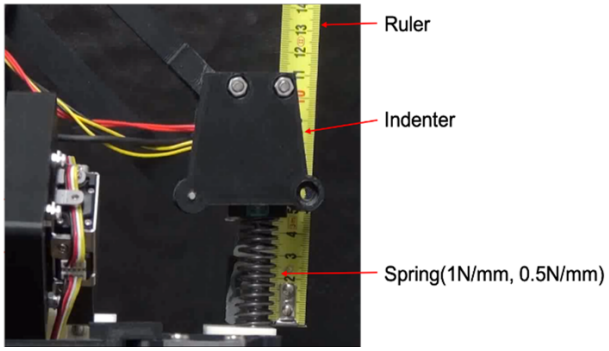

(a) experimental setup using the known springs for verification

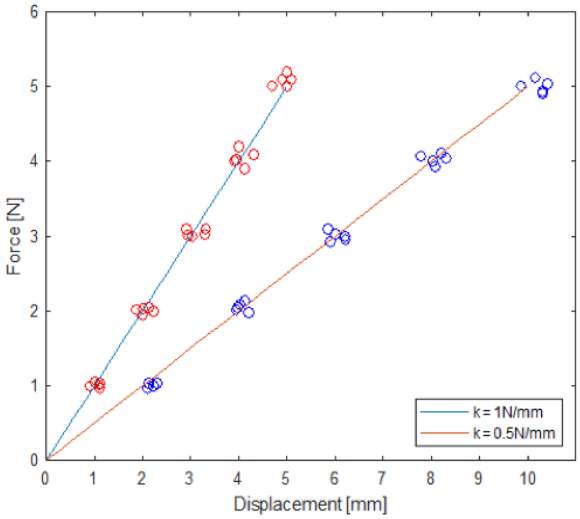

(b) measurement results of two springs five times each with 1N increment from 1N to 5N

FIGURE 10. Actual spring experiments for verification of the proposed stiffness measurement device.

forces were set to 5[N] for all indenters. The indentation displacements and forces were measured while pressing the forearm 70[mm] away from the arm anchorage part of the wrist three times each. Although all pressing force profiles reached the target forces of 5[N] at the final stages, the force profiles did not show linearities between the indentation forces and displacements as shown in Fig. 11. Now, we can calculate the average stiffnesses and their standard deviations as shown in Fig. 12 using the data obtained in Fig. 11 and the angles between the indenter axis and the direction perpendicular to the skin. Indeed, the stiffness in Fig. 12 is equivalent to the tangential slope at the specific displacements in Fig. 11. The stiffnesses at the initial displacements were relatively low but increased as expected based on the properties of human skin.

Furthermore, stiffness measurement experiments of the proposed device were repeatedly conducted with thirteen participants (11 men and 2 women; average and standard deviation of the participant age were 26.08 and 1.69 years old, respectively). The measurement locations consisted of

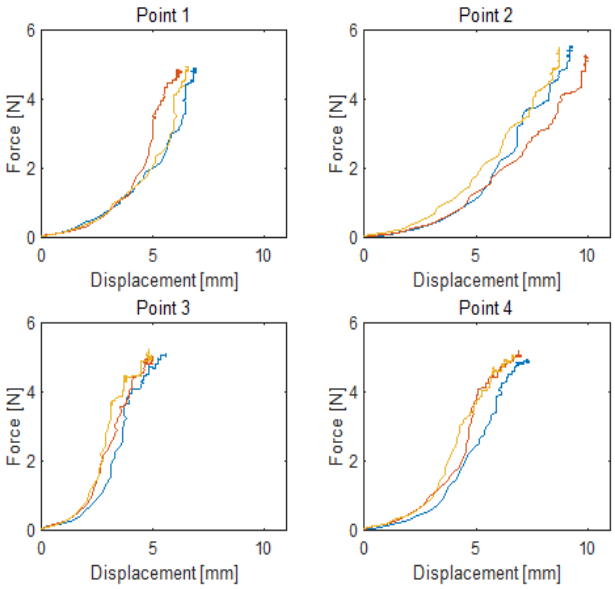

FIGURE 11. Experimental graphs between the indentation displacements and the pressing forces at four points on the human forearm. The target forces are all set to 5[N], where they were recorded three times each at the forearm region 70[mm] away from the arm anchorage part (wrist).

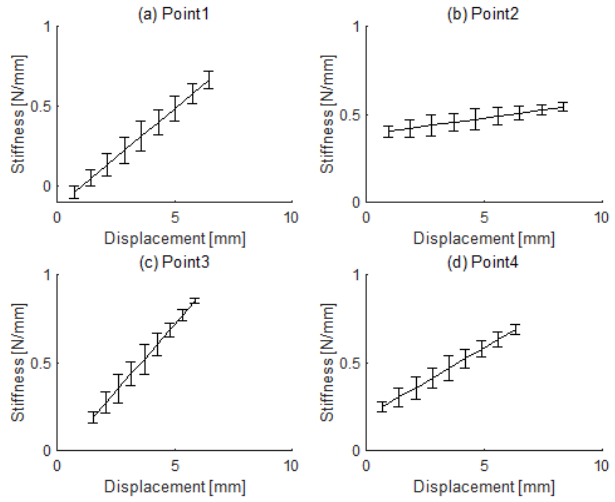

FIGURE 12. Average stiffness variations according to indentation displacements and their standard deviations calculated using the data in Fig. 11.

eight points in total, with four points at 70mm and four points at 120mm as suggested in Fig. 9(a). To further verify the repeatability of the forces measured from the human forearm, repeated-measures ANOVA (RM-ANOVA) test was performed by the repetitive measurements. As shown in Fig. 13, there were significant differences in statistics between the stiffnesses corresponding to the four points at 70mm away from the wrist ($p<.001$).

The experimental results for the thirteen participants are listed in Table 2, where the over-line notation $(\overline{\cos\theta}, \bar{k})$ represents the average values for the thirteen participants, and

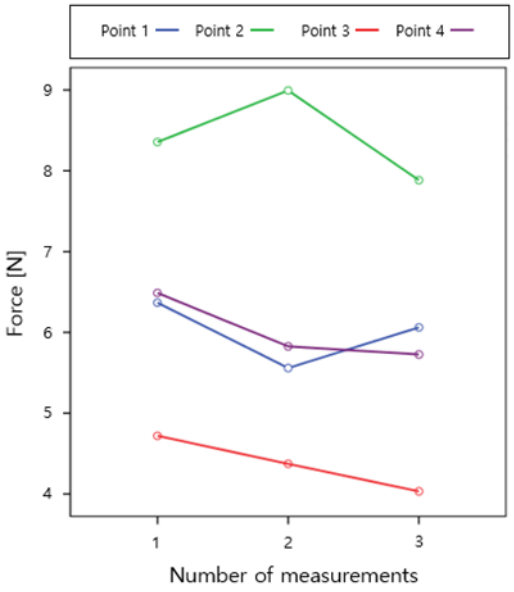

FIGURE 13. Average force according to the measurement locations (point 1 thru 4 at 70mm) in the repetitive measurements.

TABLE 2. Average stiffnesses of thirteen subjects according to the measurement locations of the forearm.

Point	Position	$\overline{\cos\theta}$	$\sigma(\cos\theta)$	$\overline{k}$ [N/mm]	$\sigma(k)$ [N/mm]
1	70[mm]	0.9934	0.0045	0.6556	0.1327
	120[mm]	0.9915	0.0274	0.5032	0.0765
2	70[mm]	0.9991	0.0194	0.4935	0.0982
	120[mm]	0.9895	0.0027	0.7620	0.1575
3	70[mm]	0.9846	0.0132	0.8237	0.0954
	120[mm]	0.9907	0.0027	0.7620	0.1575
4	70[mm]	0.9426	0.0454	0.6752	0.1441
	120[mm]	0.9911	0.0122	0.5213	0.1301

σ expresses the standard deviation of the corresponding parameter. Especially, note that the mean and standard deviation of the forearm stiffness k for thirteen participants (calculated as $k = F_\theta/x$) are given in Table 2, where x denotes the indentation displacement and F_θ denotes the force calculated by the Eq. (3). As seen in Table 2, point 3 at the 70[mm] position had the highest stiffness, while point 2 at the 70[mm] position showed the lowest. As the measurement point moves closer to the ulna, the stiffness becomes high, while movement in the opposite point results in lower stiffness.

The developed device was able to make simultaneous measurements at four points according to the circumference of forearm in one measurement cycle, unlike previous studies [11]–[14]. Further, it was possible to make measurements at various forearm locations using the parallelogram mechanism after anchoring the wrist of the participant during the experiment. For more exact measurements of the forearm stiffness, the following three factors were considered for the proposed device. First, the device was designed to operate the arm anchorage part and the measurement part in separated states, for minimizing the artifacts due to participant movement during measurement. Second, the proposed device could record both the indentation forces and displacements, after being contacted with the forearm, ultimately to accurately calculate the stiffnesses according to the circumference of forearm. Finally, our device was designed to press along the normal direction of the participant's forearm skin to decrease the skin slipperiness.

IV. CONCLUSIONS

In this paper, the stiffness measurement device of the human forearm was proposed that consisted of four indenters for the measurements and four linear servomotors for the arm anchorage. For the measurement part, the forward and inverse kinematics of the parallelogram mechanism was calculated to control the end-effector position. Also, the admittance compensator was designed to control the indentation force. Its effectiveness was verified through several experiments for accuracy and repeatability of the measurement device. As far as the authors know, existing indenters only have one DoF, but the developed device has active two DoFs. Further, the existing measurement systems were uncomfortable to measure the stiffness because the subject was required to move his/her own limb whenever the measurement skin site was changed. However, the proposed device is able to move the indenter directly toward the target skin site using the parallelogram mechanism.

Performance verification of the developed device was conducted using the commercial springs. Subsequently, this device was applied to thirteen subjects to measure the forearm stiffness. From the experimental results, we could conclude that the proposed device exhibited good repeatability. It is expected that the proposed measurement device can be utilized for personalized manufacturing of prosthetic sockets such that inconvenience, manufacturing time, and cost are all reduced. A further study is needed to visualize the stiffness measurement data of the human forearm by integrating forearm stiffness measurement data into a forearm 3D shape model. Finally, the proposed measurement device can be applied to various fields such as wearable robots and pressure clothing for humans.

REFERENCES

[1] K. Ziegler-Graham, E. J. Mackenzie, P. L. Ephraim, T. G. Travison, and R. Brookmeyer, "Estimating the prevalence of limb loss in the united states: 2005 to 2050," *Arch. Phys. Med. Rehabil.*, vol. 89, no. 3, pp. 422–429, Mar. 2008.

[2] R. D. Alley, T. W. Williams Iii, M. J. Albuquerque, and D. E. Altobelli, "Prosthetic sockets stabilized by alternating areas of tissue compression and release," *J. Rehabil. Res. Develop.*, vol. 48, no. 6, pp. 679–696, 2011.

[3] C. Lake, "The evolution of upper limb prosthetic socket design," *J. Prosthetics Orthotics*, vol. 20, no. 3, pp. 85–92, Jul. 2008.

[4] N. Herbert, D. Simpson, W. D. Spence, and W. Ion, "A preliminary investigation into the development of 3-D printing of prosthetic sockets," *J. Rehabil. Res. Develop.*, vol. 42, no. 2, p. 141, 2005.

[5] F. E. Tay, M. Manna, and L. Liu, "A CASD/CASM method for prosthetic socket fabrication using the FDM technology," *Rapid Prototyping J.*, vol. 8, no. 4, pp. 258–262, Oct. 2002.
[6] E. Biddiss, D. Beaton, and T. Chau, "Consumer design priorities for upper limb prosthetics," *Disab. Rehabil., Assistive Technol.*, vol. 2, no. 6, pp. 346–357, Jan. 2007.
[7] J. E. Sanders, E. L. Rogers, E. A. Sorenson, G. S. Lee, and D. C. Abrahamson, "CAD/CAM transtibial prosthetic sockets from central fabrication facilities: How accurate are they?" *J. Rehabil. Res. Develop.*, vol. 44, no. 3, p. 395, 2007.
[8] C. W. Moran, "Revolutionizing prosthetics 2009 modular prosthetic limb-body interface: Overview of the prosthetic socket development," *Johns Hopkins APL Tech. Dig.*, vol. 30, 2011, no. 3, pp. 250–255.
[9] H. E. J. Meulenbelt, P. U. Dijkstra, M. F. Jonkman, and J. H. B. Geertzen, "Skin problems in lower limb amputees: A systematic review," *Disability Rehabil.*, vol. 28, no. 10, pp. 603–608, Jan. 2006.
[10] J. T. Belter, J. L. Segil, A. M. Dollar, and R. F. Weir, "Mechanical design and performance specifications of anthropomorphic prosthetic hands: A review," *J. Rehabil. Res. Develop.*, vol. 50, no. 5, p. 599, 2013.
[11] A. Petron, J.-F. Duval, and H. Herr, "Multi-indenter device for *in vivo* biomechanical tissue measurement," *IEEE Trans. Neural Syst. Rehabil. Eng.*, vol. 25, no. 5, pp. 426–435, Mar. 2017.
[12] J. T. Iivarinen, R. K. Korhonen, P. Julkunen, and J. S. Jurvelin, "Experimental and computational analysis of soft tissue stiffness in forearm using a manual indentation device," *Med. Eng. Phys.*, vol. 33, no. 10, pp. 1245–1253, Dec. 2011.
[13] C. Flynn, A. Taberner, and P. Nielsen, "Measurement of the force–displacement response of in vivo human skin under a rich set of deformations," *Med. Eng. Phys.*, vol. 33, no. 5, pp. 610–619, Jun. 2011.
[14] P. Ashrafi and E. Tonuk, "Indentation and observation of anisotropic soft tissues using an indenter device," *J. Natural Appl. Sci.*, vol. 18, pp. 10–20, 2010.
[15] A. F. T. Mak, M. Zhang, and D. A. Boone, "State-of-the-art research in lower-limb prosthetic biomechanics-socket interface: A review," *J. Rehabil. Res. Develop.*, vol. 38, no. 2, pp. 161–173, 2001.
[16] S. Lee, M.-O. Kim, T. Kang, J. Park, and Y. Choi, "Knit band sensor for myoelectric control of surface EMG-based prosthetic hand," *IEEE Sensors J.*, vol. 18, no. 20, pp. 8578–8586, Oct. 2018.
[17] E. Samur, M. Sedef, C. Basdogan, L. Avtan, and O. Duzgun, "A robotic indenter for minimally invasive measurement and characterization of soft tissue response," *Med. Image Anal.*, vol. 11, no. 4, pp. 361–373, Aug. 2007.
[18] A. Pathak, M. Silver-Thorn, C. Thierfelder, and T. Prieto, "A rate-controlled indentor for in vivo analysis of residual limb tissues," *IEEE Trans. Rehab. Eng.*, vol. 6, no. 1, pp. 12–20, Mar. 1998.
[19] M. X. Kong, W. You, Z. J. Du, and L. N. Sun, "Optimal design for a 2-DOF high dynamic manipulator based on parallelogram mechanism," in *Proc. IEEE/ASME Int. Conf. Adv. Intell. Mechatronics*, Jul. 2010, pp. 242–247. doi: 10.1109/aim.2010.5695735.
[20] J. C. Shin, "Amputation and prosthesis," *Essential rehabilitation Medicine*, 2nd ed. Washington, DC, USA: Hanmibook, 2014, ch. 4, pp. 135–148.

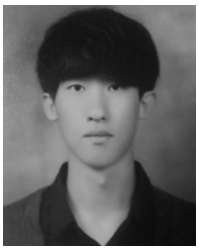

DONGHOON OH received the B.S. degree in electronic engineering from Cheongju University, South Korea, in 2017, and the M.S. degree in electrical and electronic engineering from Hanyang University, South Korea, in 2019. He is currently with Neuromeka Company.

SEULAH LEE received the M.S. and Ph.D. degrees in clothing and textiles from Hanyang University, Seoul, South Korea, in 2013 and 2017, respectively. She is currently a Postdoctoral Fellow with the Research Institute of Engineering and Technology, Hanyang University. Her current research interests include wearable sensor, smart textiles, electrodes, and smart clothing design.

YOUNGJIN CHOI (Senior Member, IEEE) was born in Seoul, South Korea, in 1970. He received the B.S. degree in precision mechanical engineering from Hanyang University, Seoul, in 1994, and the M.S. and Ph.D. degrees in mechanical engineering from POSTECH, Pohang, South Korea, in 1996 and 2002, respectively. From 2002 to 2005, he was a Senior Research Scientist with the Intelligent Robotics Research Center, Korea Institute of Science and Technology (KIST). Since 2005, he has been a Professor with the Department of Electrical and Electronic Engineering, Hanyang University, Ansan, South Korea. From 2011 to 2012, he was a Visiting Researcher with the University of Central Florida, USA. His research interests include biorobotics and control theory. From 2010 to 2014, he was an Associate Editor of the IEEE TRANSACTIONS ON ROBOTICS. From 2016 to 2018, he was an Associate Editor of the IEEE ROBOTICS AND AUTOMATION LETTERS. Since 2018, he has also been a Senior Editor of the IEEE ROBOTICS AND AUTOMATION LETTERS.